Ariumi Y, Kuroki M, Kushima Y, Osugi K, Hijikata M, Maki M, Ikeda M, Kato N.	Hepatitis C virus hijacks P-body and stress granule components around lipid droplets.	J Virol	85 (14)	6882-6892	2011
Mori K, Ikeda M, Ariumi Y, Dansako H, Wakita T, Kato N.	Mechanism of action of ribavirin in a novel hepatitis C virus replication cell system.	Virus Res	157 (1)	61-70	2011
Ueda Y, Mori K, Ariumi Y, Ikeda M, Kato N.	Plural assay systems derived from different cell lines and hepatitis C virus strains are required for the objective evaluation of anti-hepatitis C virus reagents.	Biochem Biophys Res Commun	409 (4)	663-668	2011
Ikeda M, Kawai Y, Mori K, Yano M, Abe K, Nishimura G, Dansako H, Ariumi Y, Wakita T, Yamamoto K, Kato N.	Anti-ulcer agent teprenone inhibits hepatitis C virus replication: potential treatment for hepatitis C.	Liver Int	31(6)	871-880	2011
Mori K, Ueda Y, Ariumi Y, Dansako H, Ikeda M, Kato N.	Development of a drug assay system with hepatitis C virus genome derived from a patient with acute hepatitis C.	Virus Genes		In press	2012
Osugi K, Suzuki H, Nomura T, Ariumi Y, Shibata H, Maki M.	Identification of the P-body components PATL1 as a novel ALG2-interacting protein by in silico and Far-Western screening of proline-rich proteins.	J Biochem		In press	2012
有海康雄 加藤宣之	HCVによる肝発癌機構	新時代のウイルス性肝炎学　日本臨床	69(増刊4)	64-68	2011
Saeed M, Suzuki R, Watanabe N, Masaki T, Tomonaga M, Muhammad A, Kato T, Matsuura Y, Watanabe H, Wakita	Role of the endoplasmic reticulum-associated degradation (ERAD) pathway in degradation of	J Biol Chem	286	37264-37273	2011

T, Suzuki T.	hepatitis C virus envelope proteins and production of virus particles.				
Saeed M, Shiina M, Date T, Akazawa D, Watanabe N, Murayama A, Suzuki T, Watanabe H, Hiraga N, Imamura M, Chayama K, Choi Y, Krawczynski K, Liang TJ, Wakita T, Kato T.	In vivo adaptation of hepatitis C virus in chimpanzees for efficient virus production and evasion of apoptosis.	Hepatology	54	425-433	2011
Okamoto Y, Masaki T, Murayama A, Munakata T, Nomoto A, Nakamoto S, Yokosuka O, Watanabe H, Wakita T, Kato T.	Development of recombinant hepatitis C virus with NS5A from strains of genotypes 1 and 2.	Biochem Biophys Res Commun	410	404-409	2011
Murayama A, Kato T, Akazawa D, Sugiyama N, Date T, Masaki T, Nakamoto S, Tanaka Y, Mizokami M, Yokosuka O, Nomoto A, Wakita T.	Production of infectious chimeric hepatitis C virus genotype 2b harboring minimal regions of JFH-1.	J Virol	86(4)	2143-2152	2012
Inoue H, Yamazaki S, Shimizu M, Uozaki H, Goto T, Ohnishi S, Koike K.	Liver injury induced by the Japanese herbal drug kamishoyosan.	Gastroenterol Hepatol (NY)	7(10)	692-695	2011
Arano T, Nakagawa H, Tateishi R, Ikeda H, Uchino K, Enooku K, Goto E, Masuzaki R, Asaoka Y, Kondo Y, Goto T, Shiina S, Omata M, Yoshida H, Koike K.	Serum level of adiponectin and the risk of liver cancer development in chronic hepatitis C patients.	Int J Cancer	129	2226-2235	2011
Goto T, Yoshida H, Tateishi R, Enooku K, Goto E, Sato T, Ohki T, Masuzaki R, Imamura J, Shiina	Influence of serum HBV DNA load on recurrence of hepatocellular carcinoma after	Hepatol Int	5(3)	767-773	2011

S, Koike K, Omata M.	treatment with percutaneous radiofrequency ablation.				
Kudo Y, Tanaka Y, Tateishi K, Yamamoto K, Yamamoto S, Mohri D, Isomura Y, Seto M, Nakagawa H, Asaoka Y, Tada M, Ohta M, Ijichi H, Hirata Y, Otsuka M, Ikenoue T, Maeda S, Shiina S, Yoshida H, Nakajima O, Kanai F, Omata M, Koike K.	Altered composition of fatty acids exacerbates hepatotumorigenesis during activation of the phosphatidylinositol 3-kinase pathway.	J Hepatol	55(6)	1400-1408	2011
Ishizaka N, Hongo M, Sakamoto A, Saito K, Furuta K, Koike K.	Liver lipid content is reduced in rat given 7-day administration of angiotensin II.	J Renin Angiotensin Aldosterone Syst	12(4)	462-468	2011
Bertot LC, Sato M, Tateishi R, Yoshida H, Koike K.	Mortality and complication rates of percutaneous ablative techniques for the treatment of liver tumors: a systematic review.	Eur Radiol	21 (12)	462-468	2011
Yamashiki N, Sugawara Y, Tamura S, Kaneko J, Yoshida H, Aoki T, Hasegawa K, Akahane M, Ohtomo K, Fukayama M, Koike K, Kokudo N.	Diagnostic accuracy of α-fetoprotein and des-γ-carboxy prothrombin in screening for hepatocellular carcinoma in liver transplant candidates.	Hepatol Res	41 (12)	1199-1207	2011
Fujinaga H, Tsutsumi T, Yotsuyanagi H, Moriya K, Koike K.	Hepatocarcinogenesis in hepatitis C: HCV shrewdly exacerbates oxidative stress by modulating both production and scavenging of reactive oxygen species.	Oncology	Suppl 1	11-17	2011
Ikeda H, Tateishi R, Enooku K, Yoshida H, Nakagawa H,	Prediction of hepatocellular carcinoma	Cancer Epidemiol Biomarkers Prev	20 (10)	2204-2211	2011

Masuzaki R, Kondo Y, Goto T, Shiina S, Kume Y, Tomiya T, Inoue Y, Nishikawa T, Ohtomo N, Tanoue Y, Ono T, Koike K, Yatomi Y.	development by plasma ADAMTS13 in chronic hepatitis B and C.				
Watanabe S, Enomoto N, Koike K, Izumi N, Takikawa H, Hashimoto E, Moriyasu F, Kumada H, Imawari M ; PERFECT Study Group.	Cancer preventive effect of pegylated interferon α-2b plus ribavirin in a real-life clinical setting in Japan: PERFECT interim analysis.	Hepatol Res	41 (10)	955-964	2011
Otsuka M, Takata A, Yoshikawa T, Kojima K, Kishikawa T, Shibata C, Takekawa M, Yoshida H, Omata M, Koike K.	Receptor for activated protein kinase C: requirement for efficient microRNA function and reduced expression in hepatocellular carcinoma.	PLoS One	6(9)	e24359.	2011
Uchino K, Tateishi R, Shiina S, Kanda M, Masuzaki R, Kondo Y, Goto T, Omata M, Yoshida H, Koike K.	Hepatocellular carcinoma with extrahepatic metastasis: Clinical features and prognostic factors.	Cancer	117 (19)	4475-4483	2011
Takata A, Otsuka M, Kojima K, Yoshikawa T, Kishikawa T, Yoshida H, Koike K.	MicroRNA-22 and microRNA-140 suppress NF-κB activity by regulating the expression of NF-κB coactivators.	Biochem Biophys Res Commun	411 (4)	826-831	2011
Nakagawa H, Hirata Y, Takeda K, Hayakawa Y, Sato T, Kinoshita H, Sakamoto K, Nakata W, Hikiba Y, Omata M, Yoshida H, Koike K, Ichijo H, Maeda S.	Apoptosis signal-regulating kinase 1 inhibits hepatocarcinogenesis by controlling the tumor-suppressing function of stress-activated MAPK.	Hepatology	54(1)	185-195	2011
Kojima K, Takata A, Vadnais C, Otsuka M, Yoshikawa T, Akanuma M, Kondo	MicroRNA122 is a key regulator of α-fetoprotein expression and	Nat Commun	2	338	2011

Y, Kang YJ, Kishikawa T, Kato N, Xie Z, Zhang WJ, Yoshida H, Omata M, Nepveu A, Koike K.	biologically aggressive behavior of hepatocellular carcinoma.				
Tsukada K, Sugawara Y, Kaneko J, Tamura S, Tachikawa N, Morisawa Y, Okugawa S, Kikuchi Y, Oka S, Kimura S, Yatomi Y, Makuuchi M, Kokudo N, Koike K.	Living donor liver transplantations in HIV- and hepatitis C virus-coinfected hemophiliacs: Experience in a single center.	Transplantation	91 (11)	1261-1264	2011
Koshiyama A, Ichibangase T, Moriya K, Koike K, Yazawa I, Imai K.	Liquid chromatographic separation of proteins derivatized with a fluorogenic reagent at cysteinyl residues on a non-porous column for differential proteomics analysis.	J Chromatogr A	1218 (22)	3447-3452	2011
Kumar V, Kato N, Urabe Y, Takahashi A, Muroyama R, Hosono N, Otuska M, Tateishi R, Omata M, Nakagawa H, Koike K, Kamatani N, Kubo M, Nakamura Y, Matsuda K.	Genome-wide association study identifies a susceptibility locus for HCV-induced hepatocellular carcinoma.	Nat Genet	43(5)	455-458	2011
Nakagawa H, Ikeda H, Nakamura K, Ohkawa R, Masuzaki R, Tateishi R, Yoshida H, Watanabe N, Tejima K, Kume Y, Iwai T, Suzuki A, Tomiya T, Inoue Y, Nishikawa T, Ohtomo N, Tanoue Y, Omata M, Igarashi K, Aoki J,	Autotaxin as a novel serum marker of liver fibrosis.	Clin Chim Acta	412 (13-14)	1201-1206	2011

Koike K, Yatomi Y.					
Kershenobich K, Razavi HA, Cooper CL, Alberti A, Dusheiko GM, Pol S, Zuckerman E, Koike K, Han K-H, Wallace CM, Zeuzem S, Negro F.	The global health burden of hepatitis C virus infection.	Liver Int	31 (S2)	4-17	2011
Sievert W, Altraif I, Razavi HA, Abdo A, Ahmed EA, AlOmair A, Amarapurkar D, Chen C-H, Dou X, El Khayat H, elShazly M, Esmat G, Guan R, Han K-H, Koike K, Largen A, McCaughan G, Mogawer S, Monis A, Nawaz A, Piratvisuth T, Sanai FM, Sharara AI, Sibbel S, Sood A, Suh DJ, Wallace C, Young K, Negro F.	A systematic review of hepatitis C virus epidemiology in Asia, Australia and Egypt.	Liver Int	31 (S2)	61-80	2011
Yasui K, Hashimoto E, Komorizono Y, Koike K, Arii S, Imai Y, Shima T, Kanbara Y, Saibara T, Mori T, Kawata S, Uto H, Takami S, Sumida Y, Takamura T, Kawanaka M, Okanoue T; The Japan NASH Study Group ,The Ministry of Health, Labour and Welfare of Japan.	Characteristics of patients with nonalcoholic steatohepatitis who develop hepatocellular carcinoma.	Clin Gastroenterol Hepatol	9(5)	428-433	2011
Koike K, Miyoshi H, Yotsyanagi H, Moriya K.	Effect of treatment with polynsatured fatty acids on HCV-or diet-induced fatty liver.	J Hepatol	54	1325-1326	2011

Yoshimi A, Yamamoto G, Goto T, Koike K, Kurokawa M.	Hepatocellular carcinoma in cirrhotic liver with graft-versus-host disease.	Ann Hematol		2012 Feb 9.[Epub ahead of print]	
Goto E, Masuzaki R, Tateishi R, Kondo Y, Imamura J, Goto T, Ikeda H, Akahane M, Shiina S, Omata M, Yoshida H, Koike K.	Value of post-vascular phase (Kupffer imaging) by contrast-enhanced ultrasonography using Sonazoid in the detection of hepatocellular carcinoma.	J Gastroenterol		2011 Dec 27. [Epub ahead of print]	
Shiina S, Tateishi R, Arano T, Uchino K, Enooku K, Nakagawa H, Asaoka Y, Sato T, Masuzaki R, Kondo Y, Goto T, Yoshida H, Omata M, Koike K.	Radiofrequency ablation for hepatocellular carcinoma: 10-year outcome and prognostic factors.	Am J Gastroenterol		2011 Dec 13. doi: 10.1038/ajg. 2011.425. [Epub ahead of print]	
Ohki T, Tateishi R, Akahane M, Shiina S, Yamashiki N, Mikami S, Enooku K, Goto E, Masuzaki R, Kondo Y, Goto T, Inoo S, Ohtomo K, Omata M, Yoshida H, Koike K.	Characteristics of hepatocellular carcinoma nodules newly detected by computed tomography during arteriography and arterial portography: preliminary report of a randomized controlled trial.	Hepatol Int		2011 Aug 31. [Epub ahead of print]	
Enooku K, Tateishi R, Kanai F, Kondo Y, Masuzaki R, Goto T, Shiina S, Yoshida H, Omata M, Koike K.	Evaluation of molecular targeted cancer drug by changes in tumor marker doubling times.	J Gastroenterol		2011 Sep 21. [Epub ahead of print]	
Takata A, Otsuka M, Kogiso T, Kojima K, Yoshikawa T, Tateishi R, Kato N, Shiina S, Yoshida H, Omata M, Koike K.	Direct differentiation of hepatic cells from human induced pluripotent stem cells using a limited number of cytokines.	Hepatol Int		2011 Feb 6. [Epub ahead of print]	

Ⅳ．研究成果の刊行物・別刷

JOURNAL OF VIROLOGY, Sept. 2011, p. 8556–8568 Vol. 85, No. 17
0022-538X/11/$12.00 doi:10.1128/JVI.00146-11

Hepatitis C Virus Infection Promotes Hepatic Gluconeogenesis through an NS5A-Mediated, FoxO1-Dependent Pathway[▽]

Lin Deng,[1] Ikuo Shoji,[1] Wataru Ogawa,[2] Shusaku Kaneda,[1] Tomoyoshi Soga,[3] Da-peng Jiang,[1] Yoshi-Hiro Ide,[1] and Hak Hotta[1]*

Division of Microbiology, Center for Infectious Diseases,[1] and Division of Diabetes, Metabolism and Endocrinology,[2] Kobe University Graduate School of Medicine, 7-5-1 Kusunoki-cho, Chuo-ku, Kobe 650-0017, Japan, and Institute for Advanced Biosciences, Keio University, 246-2 Mizukami, Kakuganji, Tsuruoka, Yamagata 997-0052, Japan[3]

Received 21 January 2011/Accepted 7 June 2011

Chronic hepatitis C virus (HCV) infection is often associated with type 2 diabetes. However, the precise mechanism underlying this association is still unclear. Here, using Huh-7.5 cells either harboring HCV-1b RNA replicons or infected with HCV-2a, we showed that HCV transcriptionally upregulated the genes for phosphoenolpyruvate carboxykinase (PEPCK) and glucose 6-phosphatase (G6Pase), the rate-limiting enzymes for hepatic gluconeogenesis. In this way, HCV enhanced the cellular production of glucose 6-phosphate (G6P) and glucose. PEPCK and G6Pase gene expressions are controlled by the transcription factor forkhead box O1 (FoxO1). We observed that although neither the mRNA levels nor the protein levels of FoxO1 expression were affected by HCV, the level of phosphorylation of FoxO1 at Ser319 was markedly diminished in HCV-infected cells compared to the control cells, resulting in an increased nuclear accumulation of FoxO1, which is essential for sustaining its transcriptional activity. It was unlikely that the decreased level of FoxO1 phosphorylation was mediated through Akt inactivation, as we observed an increased phosphorylation of Akt at Ser473 in HCV-infected cells compared to control cells. By using specific inhibitors of c-Jun N-terminal kinase (JNK) and reactive oxygen species (ROS), we demonstrated that HCV infection induced JNK activation via increased mitochondrial ROS production, resulting in decreased FoxO1 phosphorylation, FoxO1 nuclear accumulation, and, eventually, increased glucose production. We also found that HCV NS5A mediated increased ROS production and JNK activation, which is directly linked with the FoxO1-dependent increased gluconeogenesis. Taken together, these observations suggest that HCV promotes hepatic gluconeogenesis through an NS5A-mediated, FoxO1-dependent pathway.

Hepatitis C virus (HCV) is a small, enveloped RNA virus that belongs to the genus *Hepacivirus* of the family *Flaviviridae*, and the molecular mechanisms underlying its viral replication are currently being unraveled (40). The HCV genome encodes a single polyprotein of about 3,000 amino acids, which is cleaved by host and viral proteases to generate at least 10 viral proteins, such as core, envelope 1 (E1), E2, p7, NS2, NS3, NS4A, NS4B, NS5A, and NS5B. HCV can be classified into seven genotypes, with each genotype further classified into a number of subtypes, such as HCV-1a and HCV-1b (18, 24, 59).

HCV infects more than 120 million people worldwide (57). Persistent HCV infection causes not only liver diseases (chronic hepatitis, liver cirrhosis, and hepatocellular carcinoma) but also extrahepatic manifestations, such as type 2 diabetes (2, 11, 20, 23). While it is known that liver cirrhosis impairs the glucose metabolism of the liver, there are some reports showing that HCV-infected patients over 40 years of age have an increased risk of type 2 diabetes compared with individuals without HCV infection (43). In addition, insulin receptor substrate 1 (IRS-1)/phosphatidylinositol 3-kinase (PI3-kinase) signaling was more impaired in HCV-infected patients than in non-HCV-infected controls (3). These studies imply that HCV infection may directly predispose the host toward type 2 diabetes. However, the precise mechanisms are poorly understood.

Hepatocytes play an important role in maintaining plasma glucose homeostasis by adjusting the balance between hepatic glucose production and utilization via the gluconeogenic and glycolytic pathways, respectively. It was proposed previously that increased hepatic glucose production is a major feature of type 2 diabetes (13). It is also known that hyperglycemia and the subsequent development of type 2 diabetes mellitus result, at least in part, from impaired insulin signaling together with elevated glucagon levels (5, 19). Hepatic glucose production and utilization, physiologically opposed cascades, are regulated, at least in part, at the transcriptional level of the glucose 6-phosphatase (G6Pase) and glucokinase (GK) genes, which catalyze the last and the first rate-limiting steps in gluconeogenesis and glycolysis, respectively. A number of studies have shown that fasting/feeding (or hormones) controls the transcription of these two enzymes in the opposite directions. G6Pase transcription is negatively regulated by insulin or feeding and is markedly increased in a fasting state (62). On the other hand, GK transcription is positively regulated by insulin or feeding and markedly decreased in a fasting state (33). It has also been reported that the gene expressions of gluconeogenic and glycolytic enzymes, such as G6Pase, GK, and phosphoenolpyruvate carboxykinase (PEPCK), another rate-limiting enzyme for hepatic gluconeogenesis, are regulated by certain

* Corresponding author. Mailing address: Division of Microbiology, Center for Infectious Disease, Kobe University Graduate School of Medicine, 7-5-1 Kusunoki-cho, Chuo-ku, Kobe 650-0017, Japan. Phone: 81-78-382-5500. Fax: 81-78-382-5519. E-mail: hotta@kobe-u.ac.jp.

[▽] Published ahead of print on 22 June 2011.

TABLE 1. Sequences and positions of primers used in this study

Gene (GenBank accession no.)	Primer	Positions	PCR product (bp)
GK (M69051)	5′-GCCTCCCAAAGCATCTACCTC-3′ 5′-GCTCCACTGCCCCTCCTCACC-3′	119–139 562–542	444
G6Pase (U01120)	5′-CCTGGGGCTGGCTCTCAACTC-3′ 5′-AATAGTAGTCCTCCTCAATCC-3′	889–909 1197–1177	309
PEPCK (BC023978)	5′-CCAGGCAGTGAGGGAGTTTCT-3′ 5′-ACTGTGTCTCTTTGCTCTTGG-3′	210–230 426–406	217
FoxO1 (NM_002915)	5′-GAGGGTTAGTGAGCAGGTTAC-3′ 5′-AGTCCTTATCTACAGCAGCAC-3′	2352–2372 2568–2548	217
HCV NS5A (JF343793)	5′-AGACGTATTGAGGTCCATGC-3′ 5′-CCGCAGCGACGGTGCTGATAG-3′	6899–6918 7011–7031	133
β-Glucuronidase (M15182)	5′-ATCAAAAACGCAGAAAATACG-3′ 5′-ACGCAGGTGGTATCAGTCTTG-3′	1747–1767 1984–1964	238
GAPDH (NM_002046)	5′-GCCATCAATGACCCCTTCATT-3′ 5′-TCTCGCTCCTGGAAGATGG-3′	196–216 326–344	149

transcription factors, including forkhead box O1 (FoxO1) (26, 50, 54), hepatic nuclear factor 4α (HNF-4α) (26), Krüppel-like factor 15 (KLF15) (64), and cyclic AMP (cAMP) response element binding protein (CREB) (52, 56). The deregulation of the otherwise balanced control of hepatic glucose homeostasis would potentially lead to hyperglycemia and, eventually, type 2 diabetes.

In this study, by using Huh-7.5 cells harboring HCV-1b RNA replicons, i.e., either a subgenomic RNA replicon (SGR) or a full-genomic RNA replicon (FGR) (37), and cells infected with HCV-2a (14, 37, 39), we investigated the possible effects of HCV on glucose metabolism. We report here that HCV promotes hepatic gluconeogenesis, resulting in increased cellular glucose production in hepatocytes via an NS5A-mediated, FoxO1-dependent pathway.

MATERIALS AND METHODS

Cells, HCV RNA replicons, and virus. The human hepatoma-derived cell line Huh-7.5 (7) was kindly provided by C. M. Rice (Rockefeller University, New York, NY). The SGR and FGR were prepared by using pFK5B/2884Gly (41) (a kind gift from R. Bartenschlager, University of Heidelberg, Heidelberg, Germany) and pON/C-5B (31) (a kind gift from N. Kato, Okayama University, Okayama, Japan), respectively. The SGR and FGR cells are of polyclonal origin to avoid clonal variation. Plasmid pFL-J6/JFH1, which encodes the entire viral genome of a chimeric strain of HCV-2a (J6/JFH1) (39), was kindly provided by C. M. Rice. The HCV RNA genome was transcribed *in vitro* from pFL-J6/JFH1 and transfected into Huh-7.5 cells to yield infectious HCV particles, as described previously (14). A cell culture-adapted P-47 strain (9, 14) was used throughout the experiments. Virus infection was performed at a multiplicity of infection (MOI) of 2.0. Virus infectivity was measured by indirect immunofluorescence analysis, as described below, and expressed as cell-infecting units/ml. In some experiments, SGR and FGR cells, as well as HCV-infected cells at 5 days after virus infection, were treated with 1,000 IU/ml of alpha interferon (IFN) (Sigma Chemical, St. Louis, MO) for 10 days to eliminate HCV replication.

Plasmid construction. Expression plasmids for core, p7, NS2, NS3, NS3/4A, NS4A, NS4B, NS5A, and NS5B were reported elsewhere previously (15, 32).

Real-time quantitative RT-PCR. Total cellular RNA was isolated by using RNAiso reagent (Takara, Kyoto, Japan), and cDNA was generated by using a QuantiTect reverse transcription (RT) system (Qiagen, Valencia, CA). Real-time quantitative PCR was performed by using SYBR Premix Ex *Taq* (Takara) with SYBR green chemistry on an ABI Prism 7000 system (Applied Biosystems, Foster City, CA), as reported previously (37). β-Glucuronidase and GAPDH (glyceraldehyde-3-phosphate dehydrogenase) were used as internal controls. The primers used are shown in Table 1.

G6P production assay. Huh-7.5 cells seeded into a 10-cm dish at a density of 1.0×10^6 cells/dish were infected with HCV or left uninfected. At different time points after infection, the cells were washed twice with 5% mannitol solution and covered with methanol (1 ml) containing 25 μM (each) four internal standards (3-aminopyrolidine, L-methionine sulfone, trimesate, and 2-morpholinoethanesulfonic acid) for enzyme inactivation. The mixtures of methanol and cells were collected and mixed with Milli-Q water and chloroform at ratios of 2:1:2. Both the medium and cell sample solutions were then centrifuged at $20,000 \times g$ for 15 min, and the aqueous layers were collected for centrifugal filtration through a 5-kDa-cutoff filter at $9,000 \times g$ for 2 h. The extracted metabolites were concentrated with a centrifugal concentrator and stored at −80°C until analysis. Glucose 6-phosphate (G6P) concentrations were measured by capillary electrophoresis time-of-flight mass spectrometry (CE-TOFMS), and the results were normalized to the cell number as described previously (60, 61).

Glucose production assay. Culture medium was replaced with glucose production buffer consisting of glucose-free Dulbecco's modified Eagle's medium (DMEM) (Sigma Chemical), without phenol red, supplemented with a gluconeogenic substrate (2 mM sodium pyruvate and 20 mM sodium lactate). After 24 h of incubation, the medium was collected, and the total glucose concentration was measured by using a commercial kit (Glucose CII Test Wako; Wako Pure Chemical Industries, Osaka, Japan) and normalized to the cellular protein content. As the baseline of glucose production, glucose-free DMEM with neither sodium pyruvate nor sodium lactate was used. Glucose production via gluconeogenesis equals the total glucose production minus the baseline glucose production.

Luciferase reporter assay. The PEPCK gene promoter (position −1263/+225) and a deletion mutant (position −998/+225) were inserted into the pGL3 luciferase reporter plasmid (Promega, Madison, WI). The constructs were designated rPEPCK-P5(−1263)-pGL3basic and rPEPCK-P4(−998)-pGL3basic. pRL-CMV-Renilla (Promega), which expresses *Renilla* luciferase, was used as an internal control. Huh-7.5 cells prepared in a 12-well tissue culture plate at a density of 1.0×10^5 cells/well were transiently transfected with pRL-CMV-Renilla and rPEPCK-P5(−1263)-pGL3basic or rPEPCK-P4(−998)-pGL3basic in the presence of pEF1/NS4A, pEF1/NS5A, or a control vector (32). After 48 h, a luciferase assay was performed by using the Dual-Luciferase reporter assay system (Promega). Firefly and *Renilla* luciferase activities were measured with a Lumat LB 9501 luminometer (Berthold, Bad Wildbad, Germany). Firefly luciferase activity was normalized to *Renilla* luciferase activity for each sample.

Detection of mitochondrial ROS. Mitochondrial reactive oxygen species (ROS) production was analyzed as described previously (14). Briefly, cells seeded onto glass coverslips in a 24-well plate were incubated with 5 μM MitoSOX red (Molecular Probes, Eugene, OR) at 37°C for 10 min and then fixed with 3.7% paraformaldehyde and observed under a confocal laser scanning microscope (Carl Zeiss, Oberkochen, Germany). When needed, the fixed cells

were subjected to indirect immunofluorescence analysis to confirm HCV infection or NS5A expression, as described below.

Indirect immunofluorescence. Huh-7.5 cells seeded onto glass coverslips in a 24-well plate were infected with HCV or transfected with an NS5A expression plasmid. At 5 days postinfection (dpi) or 3 days posttransfection, the cells were fixed with 3.7% paraformaldehyde in phosphate-buffered saline (PBS) for 15 min at room temperature and permeabilized with 0.1% Triton X-100 in PBS for 15 min at room temperature. Mock-infected or empty-vector-transfected cells were similarly treated as controls for comparisons. After being washed with PBS twice, cells were consecutively stained with primary and secondary antibodies. The primary antibodies used were anti-FoxO1 rabbit monoclonal antibody (Cell Signaling Technology, Danvers, MA), anti-NS5A mouse monoclonal antibody (Chemicon International, Temecula, CA), and serum from an HCV-infected patient. Secondary antibodies used were Alexa Fluor 488-conjugated goat anti-rabbit immunoglobulin G (IgG), Alexa Fluor 594-conjugated goat anti-mouse IgG or anti-human IgG (Molecular Probes), and fluorescein isothiocyanate (FITC)-conjugated goat anti-mouse IgG or anti-human IgG (MBL, Nagoya, Japan). The stained cells were observed under a confocal laser scanning microscope (Carl Zeiss).

Cell fractionation and immunoblotting. Nuclear and cytoplasmic extracts from cells were prepared by using an NE-PER nuclear and cytoplasmic extraction reagent kit (Pierce Chemical, Rockford, IL). For immunoblotting, cells were lysed with SDS sample buffer, and equal amounts of protein were subjected to SDS-polyacrylamide gel electrophoresis and transferred onto a polyvinylidene difluoride membrane (Millipore, Bedford, MA), which was then incubated with the respective primary antibodies. The primary antibodies used were mouse monoclonal antibodies against HCV core (clone 2H9; a kind gift from T. Wakita, Department of Virology II, National Institute of Infectious Diseases, Tokyo, Japan), NS3, NS4A, NS5A, GAPDH (Chemicon), FoxO1 (Sigma Chemical), phospho-Akt (Ser473) (Cell Signaling Technology), and c-Myc (9E10; Santa Cruz Biotechnology, Santa Cruz, CA); rabbit polyclonal antibodies against phospho-FoxO1 (Ser139), Oct-1 (Santa Cruz Biotechnology), c-Jun N-terminal kinase (JNK), phospho-JNK (Thr183/Tyr185), c-Jun, phospho-c-Jun (Ser63), and Akt (Cell Signaling Technology); and goat polyclonal antibody against HSP60 (Santa Cruz Biotechnology). Horseradish peroxidase-conjugated goat anti-mouse IgG, goat anti-rabbit IgG (Molecular Probes), and donkey anti-goat IgG (Santa Cruz Biotechnology) were used to visualize the respective proteins by means of an enhanced chemiluminescence detection system (ECL; GE Healthcare, Buckinghamshire, United Kingdom).

Statistical analysis. Results were expressed as means ± standard errors of the means (SEM). Statistical significance was evaluated by analysis of variance (ANOVA) and was defined as a P value of <0.05.

RESULTS

HCV upregulates gene expression of PEPCK and G6Pase and downregulates gene expression of GK. We first examined the expression levels of the genes for the rate-limiting enzymes in hepatic gluconeogenesis, PEPCK and G6Pase, and of those for GK, which catalyzes the first step of glycolysis, by means of real-time quantitative RT-PCR analysis. We observed that the PEPCK and G6Pase genes were transcriptionally activated in SGR- and FGR-harboring cells (Fig. 1A and B, left). Similarly, the PEPCK and G6Pase genes were upregulated in HCV-infected cells in a time-dependent manner, starting from 3 or 5 days postinfection (dpi) up to 14 dpi (Fig. 1A and B, middle). On the other hand, the GK gene was transcriptionally downregulated in SGR- and FGR-harboring cells and HCV-infected cells in a time-dependent manner (Fig. 1C). It is noteworthy that the gene expressions of six glycolytic enzymes (not including GK) were observed to be upregulated in HCV-infected cells at 1 dpi (16).

When IFN treatment eliminated HCV from the cells, the observed upregulation of PEPCK and G6Pase gene expressions as well as the downregulation of GK gene expression in SGR- and FGR-harboring cells and HCV-infected cells were cancelled (Fig. 1A, B, and C, left and right). Thus, our results suggest that there was a trend toward an increase in gluconeogenesis in SGR- and FGR-harboring cells and HCV-infected cells. In subsequent studies we further examined whether or not HCV replication was correlated with gluconeogenesis.

HCV promotes cellular production of glucose and G6P. We then examined the effect of HCV on cellular glucose production. The results showed that SGR- and FGR-harboring cells and HCV-infected cells produced greater amounts of glucose than did the control cells (Fig. 2A, top and middle). IFN treatment cancelled the enhanced glucose production in SGR- and FGR-harboring cells and in HCV-infected cells (Fig. 2A, top and bottom). We also investigated the production of G6P, which is an important precursor molecule that is converted to glucose in the gluconeogenesis pathway, by means of metabolome analysis. As shown in Fig. 2B, a significantly higher level of G6P was accumulated in HCV-infected cells than in control cells. Taken together, these results indicate that HCV indeed promotes hepatic gluconeogenesis to cause hyperglycemia. In the following analyses, we examined the possible mechanisms of HCV-induced increased gluconeogenesis.

HCV suppresses FoxO1 phosphorylation at Ser319, leading to the nuclear accumulation of FoxO1. It was demonstrated previously that FoxO1 in hepatocytes enhances gluconeogenesis through the transcriptional activation of various genes, including G6Pase and PEPCK (25). To investigate the possible effects of FoxO1 on HCV-induced gluconeogenesis, we examined the gene expression levels of FoxO1 by real-time quantitative RT-PCR analysis. As shown in Fig. 3A, there was neither an upregulation nor a downregulation of FoxO1 gene expression in SGR- or FGR-harboring cells or HCV-infected cells. The FoxO1 transcription factor is controlled by various post-translational modifications, which include phosphorylation, ubiquitylation, and acetylation. The phosphorylated form of FoxO1 is exported from the nucleus and thereby loses its transcriptional function (30). We therefore examined the phosphorylation status of FoxO1 at Ser319, which is critical for FoxO1 nuclear exclusion (72). The results showed that FoxO1 phosphorylation at Ser319 was markedly suppressed in HCV-infected cells from 4 dpi up to 8 dpi, compared to that in the HCV-negative control cells (Fig. 3B, first panel), in a time-dependent manner that was roughly the inverse of the pattern observed for PEPCK and G6Pase mRNA upregulations (Fig. 1A and B) and glucose production (Fig. 2A), while the total protein expression levels of FoxO1 were unchanged (Fig. 3B, second panel). Regarding this connection, Banerjee et al. reported previously that FoxO1 phosphorylation at Ser256 was also inhibited in HCV-infected cells (4). Since FoxO1 is known to be phosphorylated by Akt so as to be exported from the nucleus and transcriptionally inactivated (38), we examined whether Akt function was suppressed through its impaired phosphorylation in HCV-infected cells. The result obtained revealed that this was not the case: Akt phosphorylation was enhanced in HCV-infected cells from 4 dpi up to 6 dpi compared with the control cells (Fig. 3B, third panel), while the total protein expression levels of Akt were comparable (Fig. 3B, fourth panel). This result is consistent with a recent observation by Burdette et al. (10) showing that the Akt phosphorylation level was elevated in HCV-infected cells. These data suggest that the observed decrease in FoxO1 phosphorylation

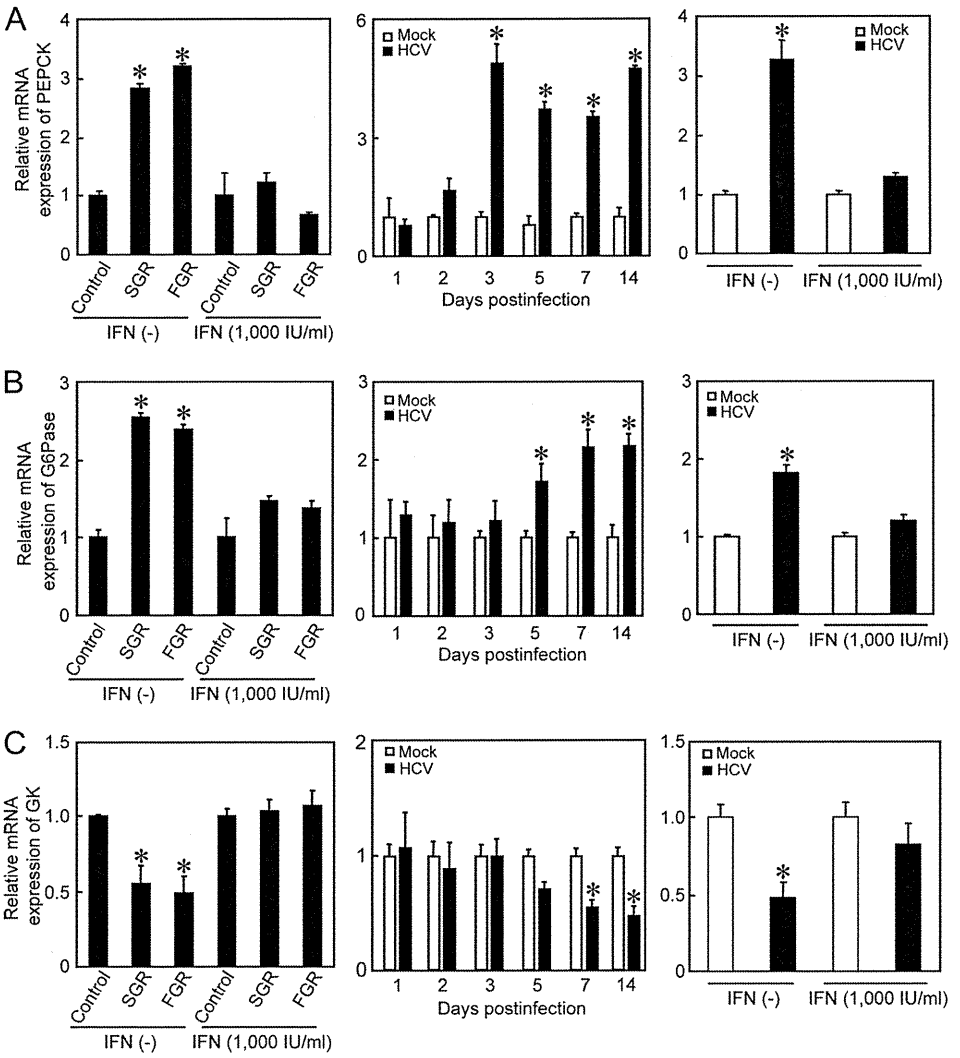

FIG. 1. HCV upregulates gene expressions of PEPCK and G6Pase and downregulates gene expression of GK. Quantitative RT-PCR analysis was performed to quantify PEPCK (A), G6Pase (B), and GK (C) mRNA expression levels in SGR- and FGR-harboring cells and HCV-infected cells (MOI = 2), and the results were normalized to β-glucuronidase mRNA expression levels. In parallel, SGR- and FGR-harboring cells and HCV-infected cells (at 5 dpi) were treated with IFN (1,000 IU/ml) for 10 days to eliminate HCV replication before being subjected to quantitative RT-PCR. Data represent means ± SEM of data from three independent experiments, and the values for the control cells were arbitrarily expressed as 1.0. *, $P < 0.01$ compared with the control.

in HCV-infected cells is caused by a mechanism independent of Akt.

Next, we tested whether HCV indeed promoted FoxO1 nuclear accumulation. The majority of FoxO1 was accumulated in the nuclear fraction in HCV-infected cells (Fig. 3C, second panel, lanes 2 and 4), whereas in control cells FoxO1 was distributed in both the nuclear and cytoplasmic fractions (lanes 1 and 3). Taken together, these results suggest that HCV suppressed FoxO1 phosphorylation, leading to the nuclear accumulation of FoxO1.

HCV-induced JNK activation is involved in the suppression of FoxO1 phosphorylation. Recent studies demonstrated that a signaling pathway that involves the stress-sensitive serine/threonine kinase JNK regulates FoxO at multiple levels (36, 66). We therefore investigated whether HCV induced JNK activation in Huh-7.5 cells. As shown in Fig. 4A, the amount of phosphorylated (activated) JNK markedly increased in HCV-infected cells in a time-dependent manner, similar to that observed for the suppression of FoxO1 phosphorylation, while the total expression levels of JNK were unchanged. As a result, c-Jun, a key substrate for JNK, was phosphorylated (activated) in HCV-infected cells but not in the mock-infected control cells. It should also be noted that the total expression levels of c-Jun in HCV-infected cells were significantly higher than those in the mock-infected control cells, suggesting that c-Jun activation through its phosphorylation stabilizes c-Jun protein expression in HCV-infected cells, as was proposed previously by Zhang et al (71).

We next sought to determine whether JNK activation was involved in the HCV-induced suppression of FoxO1 phosphorylation. HCV-infected cells at 5 days after virus infection were treated with the specific JNK inhibitor SP600125 (20 μM) (6)

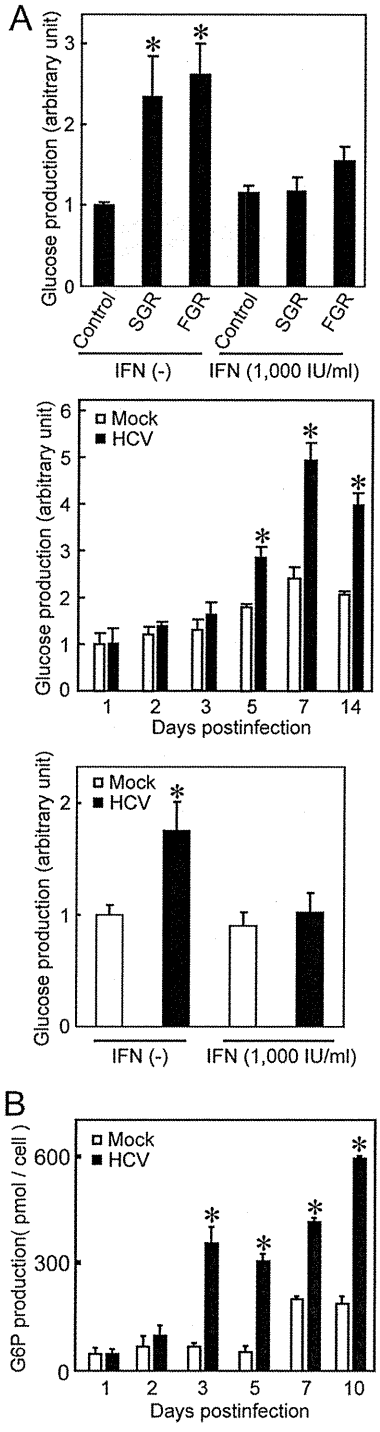

FIG. 2. HCV promotes the production of glucose and G6P. (A) Extracellular glucose production was measured in SGR- and FGR-harboring cells and HCV-infected cells (MOI = 2) and normalized to total cellular protein expression levels. In parallel, SGR- and FGR-harboring cells and HCV-infected cells (at 5 dpi) were treated with IFN (1,000 IU/ml) for 10 days to eliminate HCV replication before being subjected to glucose production analysis. Data represent means ± SEM of data from three independent experiments, and the value for the control cells was arbitrarily expressed as 1.0. *, $P < 0.01$ compared with the control. (B) Cellular G6Pase production was measured in HCV-infected cells (MOI = 2), and the results were normalized to cell numbers. Data represent means ± SEM of data from three independent experiments. *, $P < 0.01$ compared with the control.

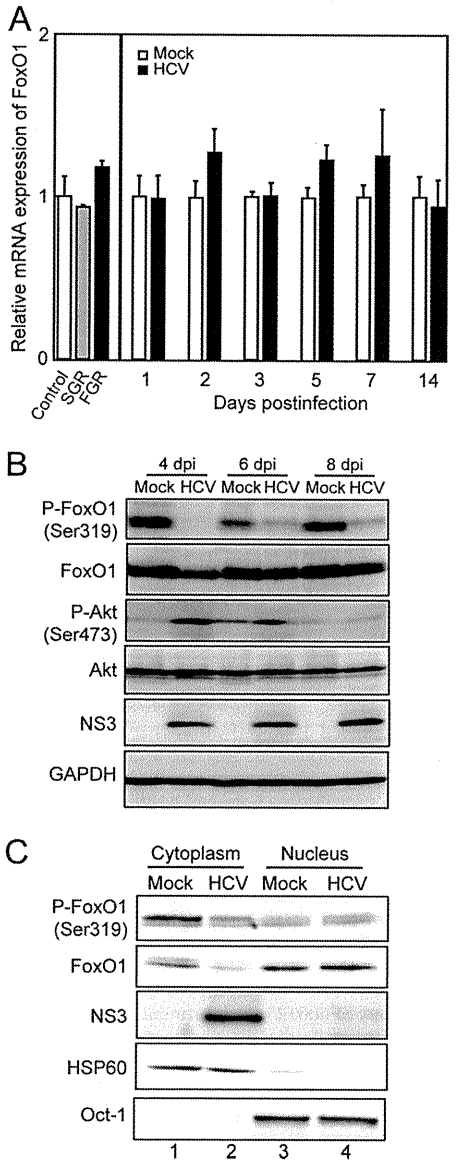

FIG. 3. HCV suppresses FoxO1 phosphorylation, leading to nuclear accumulation of FoxO1. (A) Quantitative RT-PCR analysis was performed to determine FoxO1 mRNA expression levels in SGR- and FGR-harboring cells and HCV-infected cells (MOI = 2), and expression levels were normalized to β-glucuronidase mRNA expression levels. (B) The expression levels of FoxO1, phospho-FoxO1 (Ser319) (P-FoxO1), Akt, and phospho-Akt (Ser473) were analyzed by immunoblotting of HCV-infected cells and mock-infected control cells. Blots were reprobed with antibodies recognizing NS3 and GAPDH. The amounts of GAPDH were measured as an internal control to verify equal amounts of sample loading. (C) Cytoplasmic and nuclear fractions were prepared from HCV-infected cells and mock-infected control cells at 4 dpi and were analyzed by immunoblotting using antibodies against FoxO1, phospho-FoxO1 (Ser319), NS3, Hsp60, and Oct-1. The amounts of Hsp60 and Oct-1 were measured to verify that they were equal to the amounts of cytoplasmic and nuclear fractions, respectively.

for 24 h. The catalytic JNK activity was assayed by monitoring the phosphorylation of c-Jun. As shown in Fig. 4B, SP600125 clearly prevented the phosphorylation of c-Jun and concomitantly recovered the suppression of FoxO1 phosphorylation in

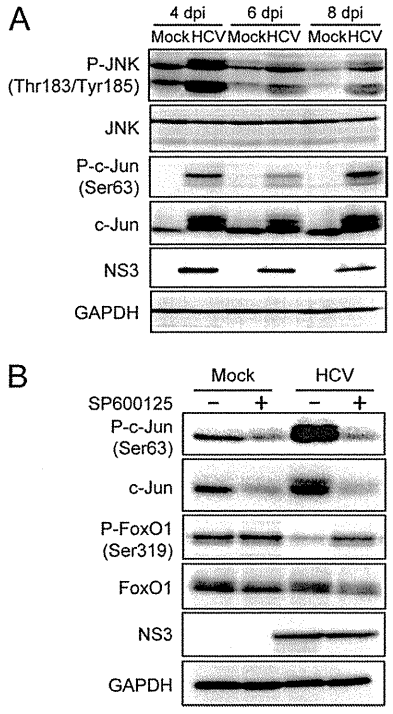

FIG. 4. HCV-induced JNK activation is required for the suppression of FoxO1 phosphorylation. (A) HCV activates the JNK/c-Jun signaling pathway. The activation (phosphorylation) of JNK (Thr183/Tyr185) and c-Jun (Ser63) in whole-cell lysates of HCV-infected cells and mock-infected control cells was analyzed by immunoblotting. Blots were reprobed with antibodies recognizing total JNK and c-Jun, NS3, and GAPDH. The amounts of GAPDH were measured as an internal control to verify equal amounts of sample loading. (B) Pretreatment with the JNK inhibitor SP600125 abrogates HCV-induced c-Jun activation and FoxO1 phosphorylation suppression. The phosphorylation of c-Jun (Ser63) and that of FoxO1 (Ser319) were analyzed by immunoblotting at 6 dpi in HCV-infected cells and mock-infected control cells with or without SP600125 pretreatment (20 μM for 24 h). Blots were reprobed with antibodies recognizing total c-Jun and FoxO1, NS3, and GAPDH. The amounts of GAPDH were measured as an internal control to verify equal amounts of sample loading.

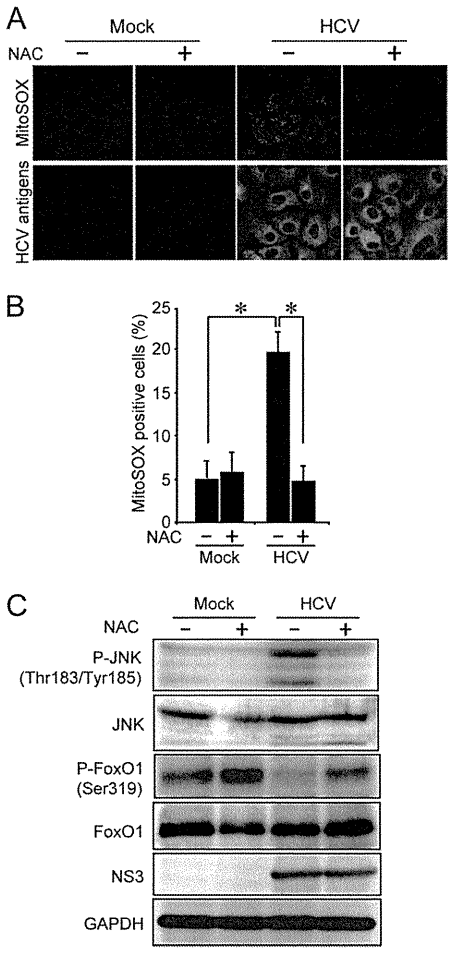

FIG. 5. HCV-induced production of mitochondrial ROS suppresses FoxO1 phosphorylation through activation of JNK. (A) Pretreatment with NAC abrogates the HCV-induced increased production of mitochondrial ROS. HCV-infected cells and mock-infected controls were pretreated with 5 mM NAC for 2 h at 6 dpi. The cells were then incubated with MitoSOX (top) and then stained for HCV antigens by using serum from an HCV-infected patient, followed by FITC-conjugated goat anti-human IgG (bottom). (B) Quantification of MitoSOX-stained cells. The percentages of cells stained with MitoSOX were determined for HCV-infected cells and mock-infected controls with or without NAC pretreatment. Data represent means ± SEM of data from two independent experiments. *, $P < 0.01$. (C) NAC pretreatment abrogates HCV-induced JNK activation and FoxO1 phosphorylation suppression. The phosphorylation of JNK (Thr183/Tyr185) and that of FoxO1 (Ser319) were analyzed by immunoblotting at 6 dpi in HCV-infected cells and mock-infected controls with or without NAC pretreatment (5 mM for 2 h). The blots were reprobed with antibodies recognizing total JNK and FoxO1, NS3, and GAPDH. The amounts of GAPDH were measured as an internal control to verify equal amounts of sample loading.

HCV-infected cells. These results suggest that HCV activates the JNK/c-Jun signaling pathway, which induces the nuclear accumulation of FoxO1 by reducing its phosphorylation status.

HCV-induced mitochondrial ROS production is involved in FoxO1 phosphorylation suppression, FoxO1 nuclear accumulation, and increased glucose production through JNK activation. We previously reported that HCV infection increases mitochondrial ROS production (14). JNK is known to be activated by ROS (35). We therefore sought to determine whether the HCV-induced increase in ROS production is an event occurring upstream of JNK activation by HCV. The pretreatment of HCV-infected cells (at 6 dpi) with 5 mM *N*-acetyl cysteine (NAC) (a general antioxidant) for 2 h significantly reduced the HCV-induced increase in ROS levels (Fig. 5A and B), as revealed by using MitoSOX, a fluorescent probe specific for superoxide that selectively accumulates in the mitochondrial compartment. As shown in Fig. 5C, NAC clearly prevented the phosphorylation of JNK and concomitantly recovered the suppression of FoxO1 phosphorylation in HCV-infected cells. These results suggest that HCV-induced ROS production is involved in JNK activation, which results in the inhibition of FoxO1 phosphorylation.

We next investigated the effects of JNK activation and ROS production on the subcellular localization of FoxO1 in HCV-infected cells by indirect immunofluorescence staining. As shown in Fig. 6A and B, FoxO1 was localized predominantly in the cytoplasm of mock-infected control cells. On the other

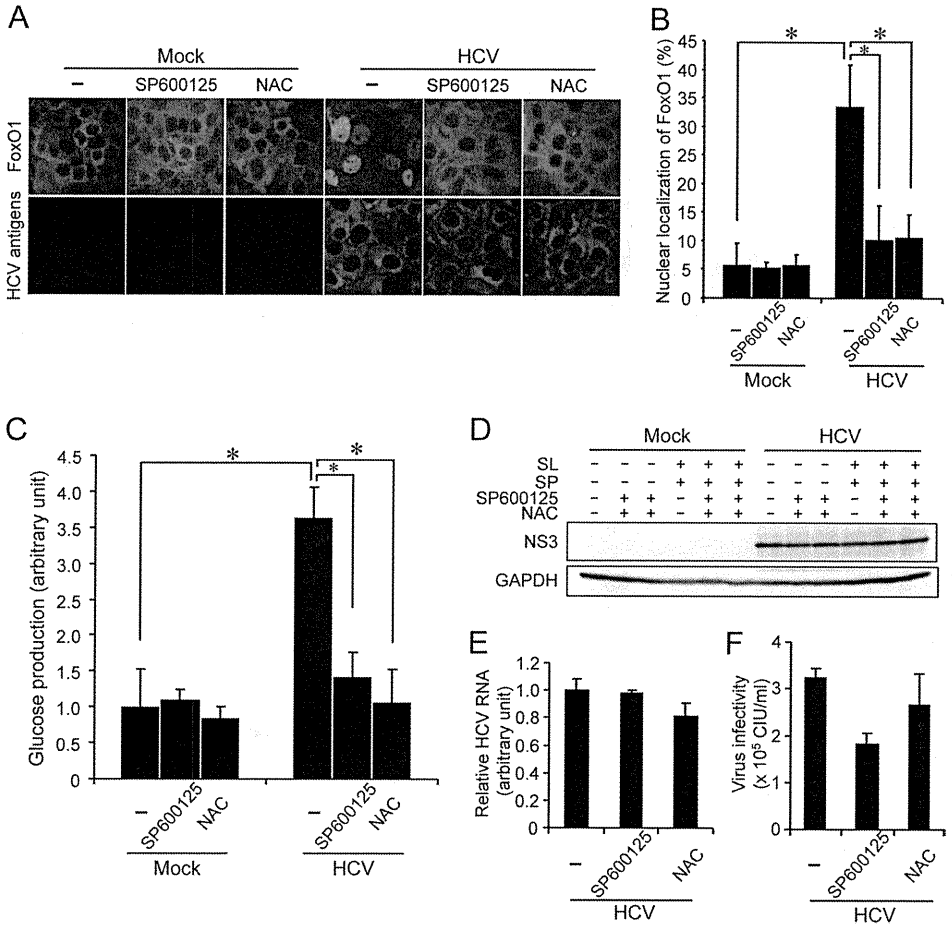

FIG. 6. HCV-induced JNK activation and ROS production are involved in FoxO1 nuclear accumulation and increased glucose production. (A) Subcellular localization of FoxO1 in HCV-infected cells and mock-infected controls with or without JNK inhibitor (SP600125 at 20 μM for 24 h) or antioxidant (NAC at 5 mM for 2 h) pretreatment at 5 dpi was examined by confocal microscopy. After fixation and permeabilization, the cells were incubated with an anti-FoxO1 rabbit monoclonal antibody followed by Alexa Fluor 488-conjugated goat anti-rabbit IgG (top) and with serum from an HCV-infected patient followed by Alexa Fluor 594-conjugated goat anti-human IgG (bottom). (B) The percentages of cells with FoxO1 nuclear localization were determined for HCV-infected cells and mock-infected controls with or without SP600125 or NAC pretreatment. Data represent means ± SEM of data from two independent experiments. *, $P < 0.01$. (C) Extracellular glucose production was measured in HCV-infected cells and mock-infected controls with or without SP600125 or NAC pretreatment at 7 dpi and normalized to total cellular protein expression levels. Data represent means ± SEM of data from two independent experiments, and the value for the control cells was arbitrarily expressed as 1.0. *, $P < 0.01$. (D) Cellular expression levels of NS3 in HCV-infected cells and mock-infected control cells with or without sodium lactate (SL), sodium pyruvate (SP), SP600125, or NAC are shown. The amounts of GAPDH were measured as an internal control to verify equal amounts of sample loading. (E) Amounts of HCV RNA were measured by quantitative RT-PCR analysis of HCV-infected cells treated with SP600125 or NAC or left untreated at 6 dpi. The amounts were normalized to GAPDH mRNA expression levels. Data represent means ± SEM of data from two independent experiments, and the value for the nontreated HCV-infected cells was arbitrarily expressed as 1.0. (F) Virus infectivity in the culture supernatants of HCV-infected cells treated with SP600125 or NAC or left untreated at 6 dpi was measured. Data represent means ± SEM of data from two independent experiments. CIU, cell-infecting units.

hand, the nuclear accumulation of FoxO1 was clearly observed in approximately 35% of HCV-infected cells at 5 dpi. The treatment of HCV-infected cells with a JNK inhibitor (SP600125 at 20 μM for 24 h) or an antioxidant (NAC at 5 mM for 2 h) significantly inhibited HCV-induced FoxO1 nuclear accumulation.

To further verify the role played by JNK activation and ROS production in HCV-induced hepatic gluconeogenesis, the glucose production in SP600125- or NAC-treated HCV-infected cells was assessed. Treatment with SP600125 or NAC significantly impaired the HCV-induced increased glucose production at 7 dpi (Fig. 6C) but did not affect the overall abundance of the HCV NS3 protein (Fig. 6D). We also examined the possible effects of SP600125 or NAC on HCV RNA replication and infectious-virus production. The results obtained revealed that treatment with SP600125 (20 μM for 24 h) or NAC (5 mM for 2 h) barely affected HCV RNA replication (Fig. 6E). On the other hand, we noted a tendency for infectious-virus production to be only slightly suppressed by SP600125 but not by NAC (Fig. 6F). A short-term inhibition of glucose production might not sufficiently affect HCV RNA replication or virus production.

Taken together, these results indicate that ROS-mediated JNK activation plays a key role in the suppression of FoxO1

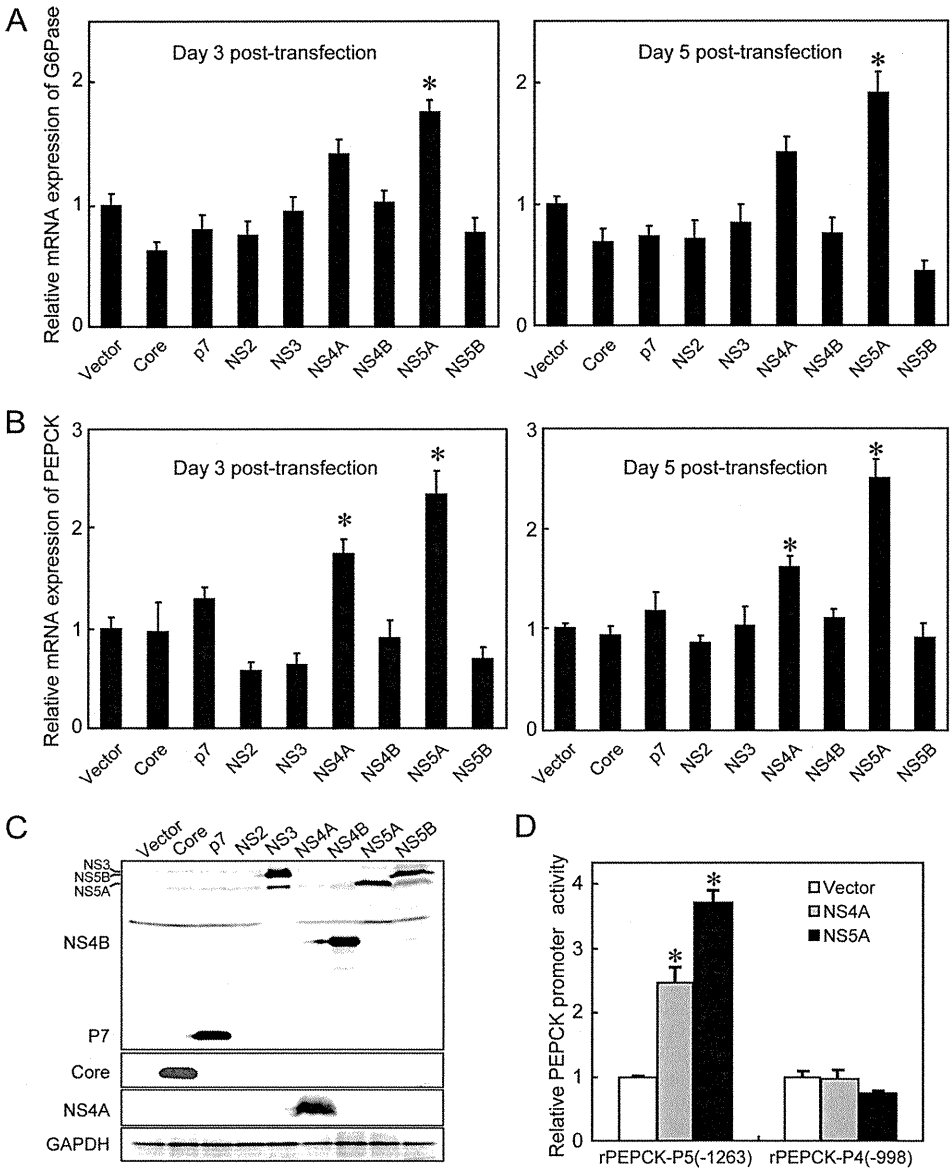

FIG. 7. HCV NS5A is involved in increased mRNA expression levels for G6Pase and PEPCK. Huh-7.5 cells were transfected with the indicated HCV viral protein expression plasmids. (A and B) At 3 and 5 days posttransfection, quantitative RT-PCR analyses of mRNA for G6Pase (A) and PEPCK (B) were conducted, and the results were normalized to β-glucuronidase mRNA expression levels. Data represent means ± SEM of data from three independent experiments, and the values for the control cells were arbitrarily expressed as 1.0. *, $P < 0.01$ compared with the control. (C) At 3 days posttransfection, the expression levels of each of the HCV proteins were examined by immunoblot analysis using antibodies against c-Myc, core, NS4A, and GAPDH. The amounts of GAPDH served as an internal control to verify equal amounts of sample loading. (D) NS5A and NS4A enhance PEPCK promoter activity. NS5A and NS4A expression plasmids were each cotransfected with rPEPCK-P5(−1263)-pGL3basic or rPEPCK-P4(−998)-pGL3basic in Huh-7.5 cells. At 48 h after transfection, the PEPCK promoter activities were measured by using a luciferase reporter assay. Data represent means ± SEM of data from three independent experiments, and the values for the control cells were arbitrarily expressed as 1.0. *, $P < 0.05$ compared with the control.

phosphorylation, the nuclear accumulation of FoxO1, and the enhancement of glucose production in HCV-infected cells.

HCV NS5A is involved in the enhancement of glucose production. To examine which HCV protein(s) is involved in the enhancement of gluconeogenesis, expression constructs of each of the HCV viral proteins were transfected into Huh-7.5 cells, and the gene expression levels of PEPCK and G6Pase were examined by real-time quantitative RT-PCR analysis. We observed that NS5A significantly promoted G6Pase gene expression (Fig. 7A). Moreover, both the NS5A and NS4A proteins significantly enhanced PEPCK gene expression at 3 and 5 days posttransfection, respectively (Fig. 7B). The expression of each of the HCV proteins except NS2 was verified by immunoblot analysis (Fig. 7C). NS2 was reported previously to be unstable and rapidly degraded by the proteasome (22).

Next, we performed a luciferase reporter assay to examine

the possible effects of NS5A and NS4A on PEPCK promoter activities. The construct rPEPCK-P5(−1263)-pGL3basic carries 1,263 bp of the PEPCK 5′-flanking region (−1263 PEPCK) and is used to monitor PEPCK promoter activity. The results demonstrated that the levels of PEPCK promoter activities were significantly higher in both NS5A- and NS4A-expressing cells than in the control cells (Fig. 7D). Interestingly, when the region of the PEPCK promoter from positions −1263 to −998 was deleted, the activation of PEPCK promoter activity in cells expressing NS5A and NS4A was abolished. These results confirmed that NS5A and NS4A activate the PEPCK promoter, leading to an increase in PEPCK mRNA expression levels. Database searches of the deleted sequence did not reveal any potential binding sequences for transcription factors (data not shown).

Recently reported data suggest that ROS production is induced in NS5A-expressing cells (17) or in hepatocytes of NS5A transgenic mice (68). We therefore sough to determine whether NS5A contributes to increased hepatic gluconeogenesis through the induction of ROS production. The NS5A expression plasmid was transfected into Huh-7.5 cells, and ROS production was assessed by MitoSOX at 3 days posttransfection. As shown in Fig. 8A and B, approximately 30% of NS5A-expressing cells displayed a much stronger signal than that observed for vector-transfected control cells.

We then examined whether NS5A mediated JNK/c-Jun activation and FoxO1 phosphorylation inhibition. The results obtained revealed that both the phosphorylation level at Ser63 and the total expression level of c-Jun were upregulated in NS5A-expressing cells compared to the control cells transfected with the vector plasmid or cells expressing the other HCV proteins (Fig. 8C and D, top two panels). Concomitantly, FoxO1 phosphorylation at Ser319 was clearly suppressed in NS5A- and NS4A-expressing cells compared to the control cells (Fig. 8C, compare lanes 6, 5, and 1, respectively, in the third panel). NS4A, a small protein of ca. 7 kDa, forms a stable complex with NS3 to function as a cofactor for NS3 serine protease and RNA helicase activities (51). We previously reported that NS4A caused mitochondrial damage when expressed alone but not when coexpressed with NS3 (47). We therefore speculated that the otherwise observed decrease in FoxO1 phosphorylation levels in NS4A-expressing cells might be canceled when NS4A is coexpressed with NS3. To verify this notion, we tested FoxO1 phosphorylation in cells coexpressing NS3 and NS4A. As had been expected, FoxO1 phosphorylation levels did not differ between NS3/4A-coexpressing cells and vector-transfected control cells (Fig. 8C, compare lanes 4 and 1, respectively).

Notably, we observed that the HCV core protein did not alter the phosphorylation status of c-Jun and FoxO1 (Fig. 8C, compare lanes 1 and 2), with the result being consistent with what was observed for gene expression levels of PEPCK and G6Pase in HCV core-expressing cells (Fig. 7A and B). These results imply that core is not primarily involved in HCV-induced increased gluconeogenesis under our experimental conditions. Similarly, other HCV nonstructural proteins, such as NS4B and NS5B, did not significantly influence the phosphorylation status of c-Jun and FoxO1 (Fig. 8D).

In order to further verify the effect of NS5A on the nuclear accumulation of FoxO1, we examined the subcellular localization of FoxO1 in NS5A-expressing cells by indirect immunofluorescence staining. As shown in Fig. 8E and F, the nuclear accumulation of FoxO1 was clearly observed for approximately 25% of NS5A-expressing cells but not the vector-transfected control. These results suggest that NS5A activates the JNK/c-Jun signaling pathway via increased ROS production, which results in the decreased phosphorylation and nuclear accumulation of FoxO1.

Finally, we examined the effects of NS5A and NS4A on glucose production. As shown in Fig. 9, the amounts of glucose were significantly increased in culture supernatants of NS5A- and NS4A-expressing cells, compared with the amounts of glucose in control cells, at 5 days posttransfection. Again, it is reasonable to assume that the observed increase in glucose production in NS4A-expressing cells might be canceled when NS4A is coexpressed with NS3.

These results collectively suggest that NS5A plays a role, at least to some extent, in the HCV-induced enhancement of hepatic gluconeogenesis.

DISCUSSION

Hepatocytes play an important role in maintaining plasma glucose homeostasis by adjusting the balance between hepatic glucose production and utilization via the gluconeogenic and glycolytic pathways, respectively. We previously reported that HCV suppresses cellular glucose uptake by downregulating the surface expression of the glucose transporters GLUT1 and GLUT2 (37). In this study, we have demonstrated that HCV promotes FoxO1-mediated hepatic gluconeogenesis, as evidenced by the increased accumulation of FoxO1 in the nucleus via the reduction of its phosphorylation status (Fig. 3 and 6A and B), which leads to increased PEPCK and G6Pase gene expression levels (Fig. 1A and B) and the subsequent upregulation of G6P and glucose production (Fig. 2). Moreover, our results indicate that HCV-induced ROS production causes JNK activation, which results in the decreased phosphorylation and nuclear accumulation of FoxO1, leading eventually to increased glucose production (Fig. 4 to 6). Our results thus suggest that FoxO1 is a prime transcription factor in the HCV-mediated progression of hepatic gluconeogenesis through an ROS/JNK-dependent mechanism, as summarized in the schema in Fig. 10. Our results also suggest that HCV NS5A plays a role in enhanced hepatic gluconeogenesis by promoting ROS production and JNK activation (Fig. 7 to 9). In line with our observations, the NS5A-mediated induction of ROS production (68) and JNK activation (49) was reported previously by other investigators.

Increasing evidence suggests that mitochondrial dysfunction is causative of insulin resistance and type 2 diabetes. Mitochondrial dysfunction causes the upregulation of PEPCK and G6Pase, leading to increased gluconeogenesis and insulin resistance (42, 46). We previously reported that HCV causes mitochondrial damage and mitochondrion-mediated apoptosis (14, 47). Our current data further support the concept that altered mitochondrial function plays a role in the development of increased glucose production in hepatocytes.

We and other groups have reported that HCV infection increases the production of mitochondrial ROS, which plays an important role in the development and progression of inflam-

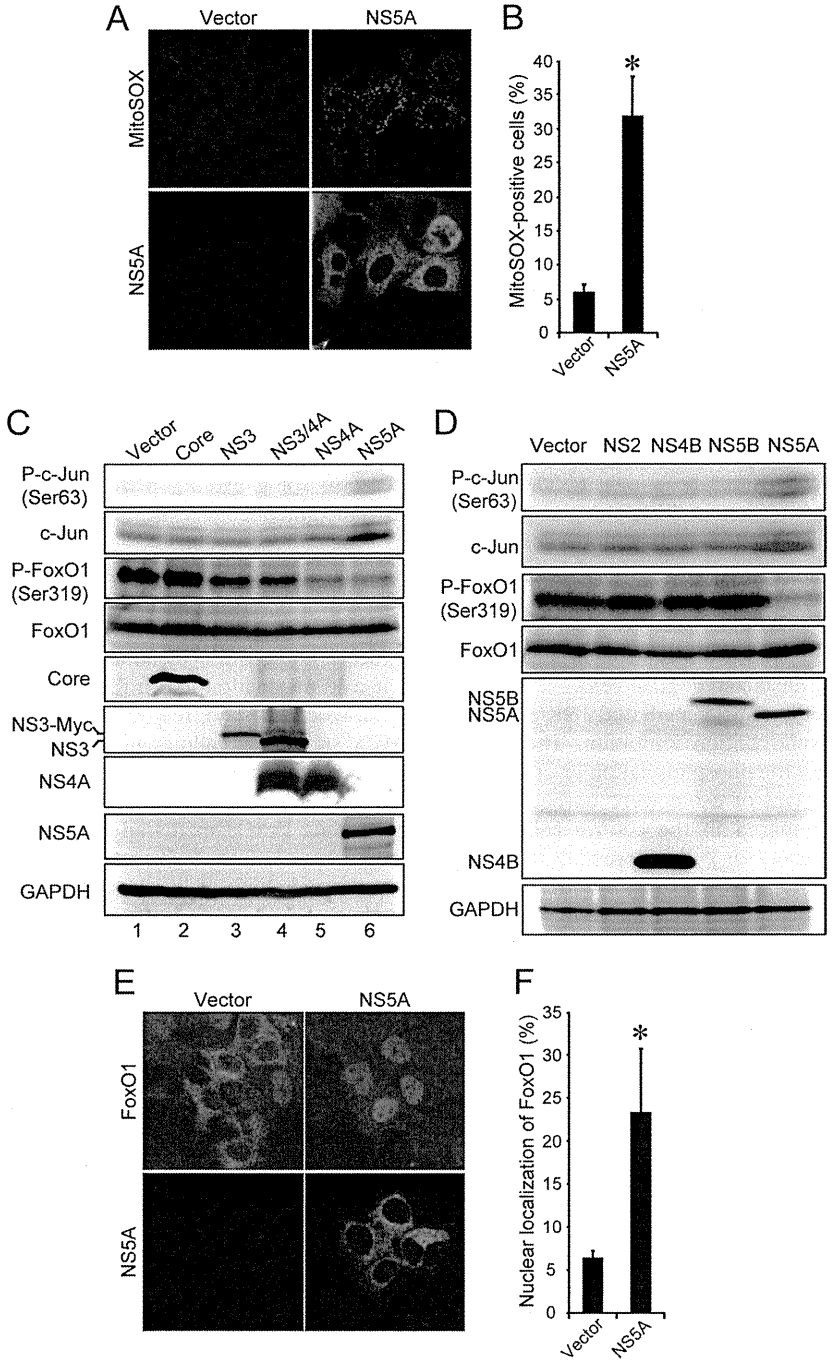

FIG. 8. HCV NS5A is involved in increased ROS production, JNK activation, FoxO1 phosphorylation suppression, and FoxO1 nuclear accumulation. (A) NS5A promotes ROS production. Huh-7.5 cells transfected with an NS5A expression plasmid or the empty control (vector) were incubated with MitoSOX (top) at 3 days posttransfection and then stained for NS5A by using anti-NS5A mouse monoclonal antibody, followed by FITC-conjugated goat anti-mouse IgG (bottom). (B) Quantification of MitoSOX-stained cells. The percentages of cells stained with MitoSOX were determined for NS5A-expressing cells and control cells. Data represent means ± SEM of data from two independent experiments. *, $P < 0.01$. (C and D) HCV NS5A activates c-Jun phosphorylation and suppresses FoxO1 phosphorylation. Huh-7.5 cells transfected with the indicated HCV viral protein expression plasmids were harvested at 3 days posttransfection, and the whole-cell lysates were subjected to immunoblot analysis using antibodies against phospho-c-Jun (Ser63), c-Jun, phospho-FoxO1 (Ser319), FoxO1, GAPDH, core, NS3, NS4A, and NS5A (C) or c-Myc (D). The amounts of GAPDH were measured as an internal control to verify equal amounts of sample loading. (E) NS5A facilitates FoxO1 nuclear accumulation. Huh-7.5 cells transfected with an NS5A expression plasmid or the empty control (vector) were fixed and permeabilized at 3 days posttransfection. The cells were incubated with an anti-FoxO1 rabbit monoclonal antibody followed by Alexa Fluor 488-conjugated goat anti-rabbit IgG (top) or with anti-NS5A mouse monoclonal antibody followed by Alexa Fluor 594-conjugated goat anti-mouse IgG (bottom). (F) The percentages of cells with a nuclear localization of FoxO1 were determined for NS5A-expressing cells and control cells. Data represent means ± SEM of data from two independent experiments. *, $P < 0.01$.

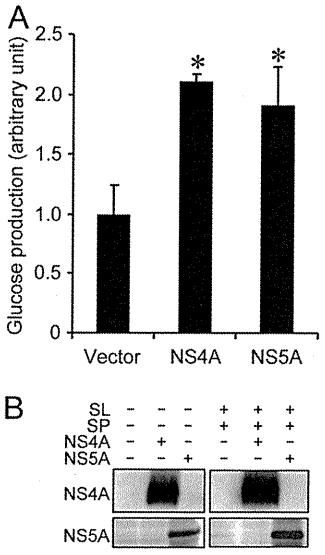

FIG. 9. HCV NS5A and NS4A enhance glucose production. (A) Huh-7.5 cells were transfected with either an NS5A or NS4A expression plasmid. At 5 days posttransfection, extracellular glucose production was measured and normalized to the total cellular protein expression level. Data represent means ± SEM of data from two independent experiments, and the values for the control cells were arbitrarily expressed as 1.0. *, $P < 0.05$ compared with the control. (B) Cellular expression levels of NS4A and NS5A in the absence and presence of sodium lactate (SL) and sodium pyruvate (SP) are shown.

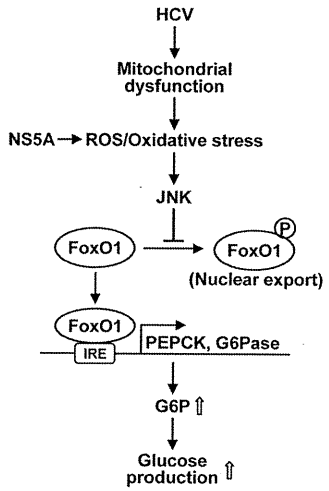

FIG. 10. Schematic representation of the HCV-dysregulated hepatic gluconeogenesis signaling pathway. HCV induces mitochondrial dysfunction (14). This results in increased ROS production and JNK activation, which induces the nuclear accumulation of FoxO1 by reducing its phosphorylation status. Consequently, PEPCK and G6Pase gene expressions are upregulated, leading to an upregulation of G6P and glucose production. NS5A plays a role in HCV-induced gluconeogenesis via the induction of ROS production. IRE, insulin response element.

matory liver disease mediated by HCV (12, 14). Increased mitochondrial ROS generation was also shown previously to be an underlying mediator of multiple forms of insulin resistance, including inflammation- or glucocorticoid-induced insulin resistance (27, 29). Moreover, a significant correlation was observed between oxidative stress and insulin resistance in patients infected with HCV genotype 1 or 2 (44). ROS have also been shown to regulate the activity of the FoxO transcription factor by posttranslational modifications, including phosphorylation (21), deacetylation (8), and ubiquitylation (67).

Although this study showed that JNK induces the nuclear accumulation of FoxO1 by reducing its phosphorylation status under oxidative stress conditions in HCV-infected cells, the precise mechanism(s) of the interplay between JNK and FoxO1 still remains to be addressed. It was reported previously that activated JNK phosphorylates IRS-1 at Ser307, which results in attenuated insulin signal transduction through the inhibition of the tyrosine phosphorylation of IRS-1 (1). Akt is a major downstream signaling protein for insulin/IRS-1 signaling and is activated through its phosphorylation on Thr308 and Ser473, the latter of which is believed to be more crucial (53). Therefore, an impairment of the insulin/IRS-1 signaling pathway should involve the downregulation of Akt phosphorylation. However, our present data showed that Akt phosphorylation on Ser473 was upregulated in HCV-infected cells at 4 and 6 dpi (Fig. 3B), suggesting that an Akt-independent pathway is involved in the JNK-mediated suppression of FoxO1 phosphorylation. Regarding this connection, it should be noted that the 14-3-3 protein, a binding partner for phosphorylated FoxO1 that mediates its nuclear export (72), is phosphorylated by JNK and that the phosphorylated 14-3-3 protein releases its binding partners, which would facilitate the nuclear accumulation of FoxO (63, 65, 70). Further studies are needed to elucidate this issue.

Another trigger that causes excessive JNK activation and insulin resistance is endoplasmic reticulum (ER) stress (28, 48). Several previous studies reported that HCV infection induces ER stress (34, 55). Under our experimental conditions, however, we did not detect significant ER stress in HCV-infected cells (14). It is thus likely that ER stress was not the primary cause of the increased gluconeogenesis in our experimental system using Huh-7.5 cells and the P-47 strain of HCV J6/JFH-1 (9, 14).

Notably, our present data showed that cells harboring the SGR or FGR and HCV-infected cells produced greater amounts of glucose than did the control cells (Fig. 2A); however, the changes in the phosphorylation status of FoxO1 and JNK in SGR- and FGR-harboring cells were not so significant compared to those in virus-infected cells (data not shown). One of the reasons for this difference is that SGR- and FGR-harboring cells were obtained through a longer cultivation in a selection medium for a month or more and that the balance of host gene induction may be somewhat different from that in virus-infected cells. Therefore, it is possible that, in addition to the JNK-FoxO1 pathway, another signaling pathway(s) is involved in the increased gluconeogenesis in SGR- and FGR-harboring cells. Studies on this issue are now under way in our laboratory.

We observed that HCV infection modulated, either positively or negatively, the transcription of the PEPCK, G6Pase, and GK genes at 3 to 5 dpi (Fig. 1). Virus infection, in general, causes dynamically changing induction and the suppression of a wide variety of host genes. For example, expression levels of certain genes, such as interferon genes, increase during an

early phase of virus infection, e.g., at 1 dpi, but return to normal levels within a few days in a cell culture system. On the other hand, the virus-infection-induced expression of other genes, such as the extracellular signal-regulated kinase (ERK) gene, remains for a prolonged period of time (data not shown). Also, some of the gene products induced in the acute phase may suppress the expression of other genes. Under these balanced conditions, it is quite possible that certain genes are induced only at a later time, e.g., 3 to 5 dpi, but not immediately after virus infection.

It was reported previously that HCV core protein-expressing transgenic mice exhibit marked insulin resistance by inhibiting IRS-1 tyrosine phosphorylation and Akt phosphorylation (45, 58). However, our present results showed that HCV NS5A, but not the core protein, was associated with increased gluconeogenesis. Moreover, it was recently reported that HCV infection significantly inhibited cellular glucose levels at 10 dpi (69), which is quite the opposite of what we observed in the present study. These results collectively suggest the possibility that multiple pathways are involved in glucose metabolism in HCV-infected cells. Also, the possible effect(s) of the dysregulation of hepatic gluconeogenesis on the HCV life cycle needs to be clarified.

In conclusion, our present results collectively suggest that HCV promotes hepatic gluconeogenesis, resulting in increased glucose production in hepatocytes via an NS5A-mediated, FoxO1-dependent pathway.

ACKNOWLEDGMENTS

We are grateful to C. M. Rice (Rockefeller University, New York, NY) for providing Huh-7.5 cells and pFL-J6/JFH1, R. Bartenschlager (University of Heidelberg, Heidelberg, Germany) for providing an HCV subgenomic RNA replicon (pFK5B/2884Gly), and N. Kato (Okayama University, Okayama, Japan) for providing an HCV full-length RNA replicon (pON/C-5B). We also thank T. Adachi (Kyoto Prefectural University of Medicine, Kyoto, Japan), K. Igarashi, K. Kashikura, and A. Suzuki (Keio University, Yamagata, Japan) for their technical assistance.

This work was supported in part by grants-in-aid for research on hepatitis from the Ministry of Health, Labor, and Welfare, Japan, and the Japan Initiative for Global Research Network on Infectious Diseases (J-GRID) program of the Ministry of Education, Culture, Sports, Science, and Technology, Japan. This study was also carried out as part of the Global Center of Excellence program of the Kobe University Graduate School of Medicine and the Science and Technology Research Partnership for Sustainable Development (SATREPS) program of the Japan Science and Technology Agency (JST) and the Japan International Cooperation Agency (JICA).

REFERENCES

1. **Aguirre, V., T. Uchida, L. Yenush, R. Davis, and M. F. White.** 2000. The c-Jun NH(2)-terminal kinase promotes insulin resistance during association with insulin receptor substrate-1 and phosphorylation of Ser(307). J. Biol. Chem. **275:**9047–9054.
2. **Alaei, M., and F. Negro.** 2008. Hepatitis C virus and glucose and lipid metabolism. Diabetes Metab. **34:**692–700.
3. **Aytug, S., D. Reich, L. E. Sapiro, D. Bernstein, and N. Begum.** 2003. Impaired IRS-1/PI3-kinase signaling in patients with HCV: a mechanism for increased prevalence of type 2 diabetes. Hepatology **38:**1384–1392.
4. **Banerjee, A., K. Meyer, B. Mazumdar, R. B. Ray, and R. Ray.** 2010. Hepatitis C virus differentially modulates activation of forkhead transcription factors and insulin-induced metabolic gene expression. J. Virol. **84:**5936–5946.
5. **Baron, A. D., L. Schaeffer, P. Shragg, and O. G. Kolterman.** 1987. Role of hyperglucagonemia in maintenance of increased rates of hepatic glucose output in type II diabetics. Diabetes **36:**274–283.
6. **Bennett, B. L., et al.** 2001. SP600125, an anthrapyrazolone inhibitor of Jun N-terminal kinase. Proc. Natl. Acad. Sci. U. S. A. **98:**13681–13686.
7. **Blight, K. J., J. A. McKeating, and C. M. Rice.** 2002. Highly permissive cell lines for subgenomic and genomic hepatitis C virus RNA replication. J. Virol. **76:**13001–13014.
8. **Brunet, A., et al.** 2004. Stress-dependent regulation of FOXO transcription factors by the SIRT1 deacetylase. Science **303:**2011–2015.
9. **Bungyoku, Y., et al.** 2009. Efficient production of infectious hepatitis C virus with adaptive mutations in cultured hepatoma cells. J. Gen. Virol. **90:**1681–1691.
10. **Burdette, D., M. Olivarez, and G. Waris.** 2010. Activation of transcription factor Nrf2 by hepatitis C virus induces the cell-survival pathway. J. Gen. Virol. **91:**681–690.
11. **Caronia, S., et al.** 1999. Further evidence for an association between non-insulin-dependent diabetes mellitus and chronic hepatitis C virus infection. Hepatology **30:**1059–1063.
12. **Choi, J., and J. H. Ou.** 2006. Mechanisms of liver injury. III. Oxidative stress in the pathogenesis of hepatitis C virus. Am. J. Physiol. Gastrointest. Liver Physiol. **290:**G847–G851.
13. **Clore, J. N., J. Stillman, and H. Sugerman.** 2000. Glucose-6-phosphatase flux in vitro is increased in type 2 diabetes. Diabetes **49:**969–974.
14. **Deng, L., et al.** 2008. Hepatitis C virus infection induces apoptosis through a Bax-triggered, mitochondrion-mediated, caspase 3-dependent pathway. J. Virol. **82:**10375–10385.
15. **Deng, L., et al.** 2006. NS3 protein of hepatitis C virus associates with the tumour suppressor p53 and inhibits its function in an NS3 sequence-dependent manner. J. Gen. Virol. **87:**1703–1713.
16. **Diamond, D. L., et al.** 2010. Temporal proteome and lipidome profiles reveal hepatitis C virus-associated reprogramming of hepatocellular metabolism and bioenergetics. PLoS Pathog. **6:**e1000719.
17. **Dionisio, N., et al.** 2009. Hepatitis C virus NS5A and core proteins induce oxidative stress-mediated calcium signalling alterations in hepatocytes. J. Hepatol. **50:**872–882.
18. **Doi, H., C. Apichartpiyakul, K. I. Ohba, M. Mizokami, and H. Hotta.** 1996. Hepatitis C virus (HCV) subtype prevalence in Chiang Mai, Thailand, and identification of novel subtypes of HCV major type 6. J. Clin. Microbiol. **34:**569–574.
19. **Dunning, B. E., and J. E. Gerich.** 2007. The role of alpha-cell dysregulation in fasting and postprandial hyperglycemia in type 2 diabetes and therapeutic implications. Endocr. Rev. **28:**253–283.
20. **Eslam, M., M. A. Khattab, and S. A. Harrison.** 2011. Insulin resistance and hepatitis C: an evolving story. Gut **60:**1139–1151.
21. **Essers, M. A., et al.** 2004. FOXO transcription factor activation by oxidative stress mediated by the small GTPase Ral and JNK. EMBO J. **23:**4802–4812.
22. **Franck, N., J. Le Seyec, C. Guguen-Guillouzo, and L. Erdtmann.** 2005. Hepatitis C virus NS2 protein is phosphorylated by the protein kinase CK2 and targeted for degradation to the proteasome. J. Virol. **79:**2700–2708.
23. **Galossi, A., R. Guarisco, L. Bellis, and C. Puoti.** 2007. Extrahepatic manifestations of chronic HCV infection. J. Gastrointestin. Liver Dis. **16:**65–73.
24. **Gottwein, J. M., et al.** 2009. Development and characterization of hepatitis C virus genotype 1-7 cell culture systems: role of CD81 and scavenger receptor class B type I and effect of antiviral drugs. Hepatology **49:**364–377.
25. **Gross, D. N., A. P. van den Heuvel, and M. J. Birnbaum.** 2008. The role of FoxO in the regulation of metabolism. Oncogene **27:**2320–2336.
26. **Hirota, K., et al.** 2008. A combination of HNF-4 and Foxo1 is required for reciprocal transcriptional regulation of glucokinase and glucose-6-phosphatase genes in response to fasting and feeding. J. Biol. Chem. **283:**32432–32441.
27. **Hoehn, K. L., et al.** 2009. Insulin resistance is a cellular antioxidant defense mechanism. Proc. Natl. Acad. Sci. U. S. A. **106:**17787–17792.
28. **Hotamisligil, G. S.** 2005. Role of endoplasmic reticulum stress and c-Jun NH2-terminal kinase pathways in inflammation and origin of obesity and diabetes. Diabetes **54**(Suppl. 2)**:**S73–S78.
29. **Houstis, N., E. D. Rosen, and E. S. Lander.** 2006. Reactive oxygen species have a causal role in multiple forms of insulin resistance. Nature **440:**944–948.
30. **Huang, H., and D. J. Tindall.** 2007. Dynamic FoxO transcription factors. J. Cell Sci. **120:**2479–2487.
31. **Ikeda, M., et al.** 2005. Efficient replication of a full-length hepatitis C virus genome, strain O, in cell culture, and development of a luciferase reporter system. Biochem. Biophys. Res. Commun. **329:**1350–1359.
32. **Inubushi, S., et al.** 2008. Hepatitis C virus NS5A protein interacts with and negatively regulates the non-receptor protein tyrosine kinase Syk. J. Gen. Virol. **89:**1231–1242.
33. **Iynedjian, P. B., et al.** 1989. Differential expression and regulation of the glucokinase gene in liver and islets of Langerhans. Proc. Natl. Acad. Sci. U. S. A. **86:**7838–7842.
34. **Joyce, M. A., et al.** 2009. HCV induces oxidative and ER stress, and sensitizes infected cells to apoptosis in SCID/Alb-uPA mice. PLoS Pathog. **5:**e1000291.
35. **Kamata, H., et al.** 2005. Reactive oxygen species promote TNFalpha-induced death and sustained JNK activation by inhibiting MAP kinase phosphatases. Cell **120:**649–661.
36. **Karpac, J., and H. Jasper.** 2009. Insulin and JNK: optimizing metabolic homeostasis and lifespan. Trends Endocrinol. Metab. **20:**100–106.
37. **Kasai, D., et al.** 2009. HCV replication suppresses cellular glucose uptake